

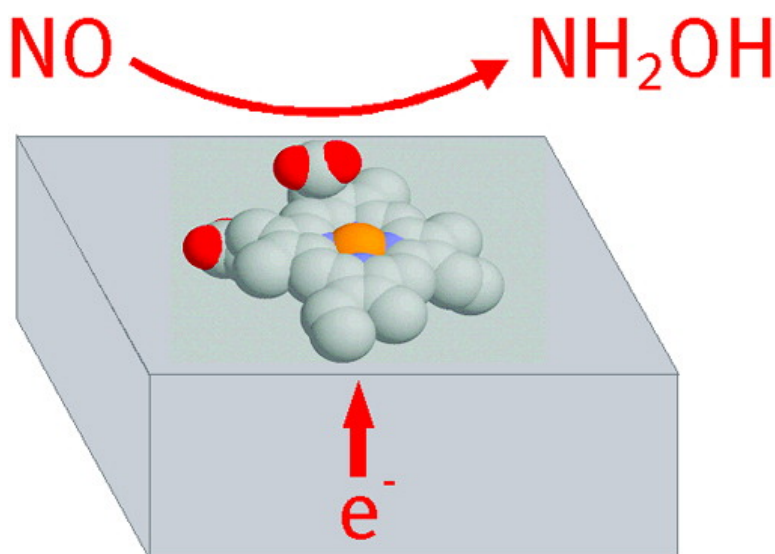
Article

Electrochemical Reduction of NO by Hemin Adsorbed at Pyrolytic Graphite

Matheus T. de Groot, Maarten Merkx, Ad H. Wonders, and Marc T. M. Koper

J. Am. Chem. Soc., **2005**, 127 (20), 7579-7586 • DOI: 10.1021/ja051151a • Publication Date (Web): 30 April 2005

Downloaded from <http://pubs.acs.org> on March 25, 2009



More About This Article

Additional resources and features associated with this article are available within the HTML version:

- Supporting Information
- Links to the 4 articles that cite this article, as of the time of this article download
- Access to high resolution figures
- Links to articles and content related to this article
- Copyright permission to reproduce figures and/or text from this article

[View the Full Text HTML](#)

Electrochemical Reduction of NO by Hemin Adsorbed at Pyrolytic Graphite

Matheus T. de Groot,[†] Maarten Merckx,[‡] Ad H. Wonders,[†] and Marc T. M. Koper^{*†}

Contribution from the Laboratory of Inorganic Chemistry and Catalysis, Schuit Institute of Catalysis and Laboratory of Macromolecular and Organic Chemistry, Department of Biomedical Engineering, Eindhoven University of Technology, P. O. Box 513, 5600 MB Eindhoven, Netherlands

Received February 23, 2005; Revised Manuscript Received March 24, 2005; E-mail: m.t.m.koper@tue.nl

Abstract: The mechanism of the electrochemical reduction of nitric oxide (NO) by hemin adsorbed at pyrolytic graphite was investigated. The selectivity of NO reduction was probed by combining the rotating ring disk electrode (RRDE) technique with a newly developed technique called on-line electrochemical mass spectroscopy (OLEMS). These techniques show that NO reduction by adsorbed heme groups results in production of hydroxylamine (NH₂OH) with almost 100% selectivity at low potentials. Small amounts of nitrous oxide (N₂O) were only observed at higher potentials. The rate-determining step in NO reduction most likely consists of an electrochemical equilibrium involving a proton transfer, as can be derived from the Tafel slope value of 62 mV/dec and the pH dependence of -42 mV/pH. The almost 100% selectivity toward NH₂OH distinguishes this system both from NO reduction on bare metal electrodes, which often yields NH₃, and from biological NO reduction in cytochrome P450nor, which yields N₂O exclusively.

Introduction

Reduction of nitric oxide (NO) to nitrous oxide (N₂O) is a key step in denitrification, the five-electron reduction of NO₃⁻ to N₂ that is used by many microorganisms to respire anaerobically and gain energy for cell growth.^{1,2} Enzymes involved in NO reduction direct the selectivity of this reaction toward N₂O (fungal cytochrome P450nor) and circumvent reduction to NH₂OH and NH₃, products that are observed in NO reduction on transition metals such as platinum^{3,4} and palladium.⁵ Understanding what controls the selectivity of NO reduction is not only interesting from a fundamental point of view, but such knowledge may also be applied to develop new catalysts for the removal of pollutants from exhaust gases, the purification of groundwater, or the more efficient production of NH₂OH, which is a raw material in nylon production.⁶

The mechanism of electrocatalytic reduction of NO by transition metals and adsorbed inorganic complexes has been extensively studied. On transition metals such as Pt^{3,4} and Pd⁵, it was found that the mechanism and the selectivity of the NO reduction depend on the kind of metal used and on the applied potential. In general, N₂O and N₂ are formed at positive

potentials, while NH₂OH and NH₃ are formed at more negative potentials. Electrochemical NO reduction on adsorbed inorganic complexes such as iron-phthalocyanine,⁶ cobalt-phthalocyanine,⁷ vitamin B12,⁸ Prussian blue,⁹ and a cobalt porphyrin¹⁰ primarily leads to the formation of NH₂OH and NH₃, with the actual selectivity depending on the specific system studied and the applied potential.

Biological NO reduction catalyzed by NO reductases such as cytochrome P450nor results in the selective formation of N₂O. This enzyme is found in the denitrifying fungus *Fusarium oxysporum*¹¹ and contains one heme group as cofactor. Reduction of NO by cytochrome P450nor^{12,13} occurs by binding of NO to the heme group, which is followed by a direct hydride transfer from NADH to the heme group,^{14,15} leading to the formation of an Fe^{II}-HNO adduct. The Fe^{II}-HNO adduct reacts with another NO molecule to form N₂O exclusively. Interestingly, a similar Fe^{II}-HNO intermediate has been proposed for the six-electron reduction of nitrite to NH₃ by the enzyme cytochrome *c'* nitrite reductase. In contrast to the cytochrome P450nor, in this multiheme enzyme (five hemes per protein),

[†] Schuit Institute of Catalysis.

[‡] Department of Biomedical Engineering.

(1) Averill, B. A. *Chem. Rev.* **1996**, *96*, 2951–2964.

(2) Wasser, I. M.; de Vries, S.; Moenne-Loccoz, P.; Schroeder, I.; Karlin, K. D. *Chem. Rev.* **2002**, *102*, 1201–1234.

(3) de Vooy, A. C. A.; Koper, M. T. M.; van Santen, R. A.; van Veen, J. A. R. *Electrochim. Acta* **2001**, *46*, 923–930.

(4) Janssen, L. J. J.; Pieterse, M. M. J.; Barendrecht, E. *Electrochim. Acta* **1977**, *22*, 27–30.

(5) de Vooy, A. C. A.; Koper, M. T. M.; van Santen, R. A.; van Veen, J. A. R. *J. Catal.* **2001**, *202*, 387–394.

(6) Otsuka, K.; Sawada, H.; Yamanaka, I. *J. Electrochem. Soc.* **1996**, *143*, 3491–3497.

(7) Ogura, K.; Yamasaki, S. *J. Appl. Electrochem.* **1985**, *15*, 279–284.

(8) Vilakazi, S. L.; Nyokong, T. *Electrochim. Acta* **2000**, *46*, 453–461.

(9) Pan, K. C.; Chuang, C. S.; Cheng, S. H.; Su, Y. O. *J. Electroanal. Chem.* **2001**, *501*, 160–165.

(10) Cheng, S.-H.; Su, Y. O. *Inorg. Chem.* **1994**, *33*, 5847–5854.

(11) Shoun, H.; Sudo, Y.; Seto, Y.; Beppu, T. *J. Biochem.* **1983**, *94*, 1219–1229.

(12) Daiber, A.; Nauser, T.; Takaya, N.; Kudo, T.; Weber, P.; Hultschig, C.; Shoun, H.; Ullrich, V. *J. Inorg. Biochem.* **2002**, *88*, 343–352.

(13) Obayashi, E.; Tsukamoto, K.; Adachi, S.-i.; Takahashi, S.; Nomura, M.; Iizuka, T.; Shoun, H.; Shiro, Y. *J. Am. Chem. Soc.* **1997**, *119*, 7807–7816.

(14) Shimizu, H.; Park, S. Y.; Lee, D. S.; Shoun, H.; Shiro, Y. *J. Inorg. Biochem.* **2000**, *81*, 191–205.

(15) Kudo, T.; Takaya, N.; Park, S.-Y.; Shiro, Y.; Shoun, H. *J. Biol. Chem.* **2001**, *276*, 5020–5026.

the Fe^{II}—HNO is further reduced to hydroxylamine and finally dehydrated to form ammonia.¹⁶

To understand the factors that govern the activity and selectivity in NO reduction by enzymes and inorganic systems, it would be interesting to study the behavior of NO reducing enzymes or their cofactors that are directly adsorbed on electrodes. In these systems, the oxidation state of the cofactor can be controlled directly by the potential applied to the electrode,^{17,18} which is very helpful in gaining mechanistic understanding of NO reduction. Unfortunately, until now, no successful immobilization of the P450nor has been achieved, but immobilization has been reported for other heme proteins such as myoglobin and hemoglobin.^{19–22} Although these heme proteins are not NO reductases, they are capable of electrochemically reducing NO when they are immobilized. N₂O was reported as the major product of electrochemical NO reduction by myoglobin,²³ hemoglobin,²⁴ and cytochrome P450 CYP119²⁵ as was shown by analysis of the head gas above the solution with a mass spectrometer.^{23,25} Analysis of the solution after NO reduction showed that NH₂OH and NH₃ were not formed in NO reduction by immobilized myoglobin.²³ In general, the mechanisms proposed for electrochemical NO reduction by immobilized myoglobin, hemoglobin, and cytochrome P450 CYP119 resemble the NO reduction mechanism for cytochrome P450nor, the only difference being that electrons for the NO reduction are not provided by NADH but by the electrode.

To provide an intermediate system between NO reduction on bare metal electrodes and enzymes immobilized on electrodes, we decided to study the electrochemical NO reduction by adsorbed heme groups (iron protoporphyrin IX). This system combines the cofactor used by enzymatic systems with the direct electronic contact between the electroactive group and the electrode typical of an (inorganic) electrochemical system. Heme groups are known to adsorb rapidly on graphite surfaces, and their electrochemical and spectroscopic properties on these surfaces have been studied extensively.^{26–36} They form an ordered structure²⁶ in which the heme groups are slightly tilted²⁷

and catalytic reactivity has been reported toward oxygen,^{28,29} hydrogen peroxide,^{29,30} organohalides,³¹ nitrite,^{32,33} and NO.^{33–36} Previous papers on NO reduction by heme adsorbed on graphite mainly focused on the development of a biosensor, however, and did not address the mechanism and selectivity of the NO reduction. Given the importance of selectivity issues in NO reduction, we have applied two techniques that are able to directly determine the selectivity of the NO reduction: on-line electrochemical mass spectrometry (OLEMS) and the rotating ring disk electrode (RRDE). OLEMS is a new technique recently developed in our laboratory that is able to measure on-line gases formed at an immersed electrode. It resembles differential electrochemical mass spectrometry (DEMS)³⁷ but has the advantage that it can be applied to electrodes of any shape and any material. OLEMS can be used very effectively in NO reduction to follow the formation of N₂O and N₂ as well as the consumption of NO, whereas the RRDE can detect the formation of NH₂OH. These techniques have a short response time, a low detection limit, are generally not influenced by reactions in solution, and can give quantitative information. Therefore, they are more effective than ex situ determinations such as sampling of the head gas or analysis of the solution, techniques that have high detection limits and can be influenced by homogeneous reactions.

Experimental Procedures

Materials. Hemin (Fluka, 98%) was used as received. All other chemicals were p.a. grade (Merck). Pyrolytic graphite (Carbone-Lorraine) was fabricated into homemade rotating ring disk electrodes.^{38,39} The geometric surface area of the electrodes was 0.5 cm². Buffer solutions were prepared with sodium acetate (pH 4–6), sodium dihydrogen phosphate monohydrate (pH 2–3, 6–8, 11–12), or boric acid (pH 9–10) combined with concentrated solutions of hydrochloric acid or caustic soda and Millipore MilliQ water (resistivity > 18.2 MΩ cm). The concentration of the buffer was 0.5 M in experiments involving NO or NH₂OH reduction and 0.1 M in all other experiments. Prior to entering the electrochemical cell, nitric oxide 2.5 (Linde AG) was bubbled through two washing flasks filled with a 3 M KOH solution, a procedure that was found to be important to remove NO₂.^{3,38} Purging the solution with NO for 10 min resulted in a saturated NO solution, which corresponds to a concentration of 2 mM as can be calculated from the Henry's Law constant of 2.0 × 10⁻³ mol atm⁻¹ at 21 °C.⁴⁰

Electrochemical Apparatus and Procedures. An Autolab PGstat 20 potentiostat was used for cyclic voltammetry. A homemade three-electrode cell consisting of a platinum flag counter electrode, a Hg|Hg₂-SO₄ or Ag|AgCl reference electrode, and a rotating ring disk electrode were used. All potentials in this paper are relative to the standard calomel electrode (SCE). The rotating ring disk electrode consisted of a pyrolytic graphite (PG) disk and a Pt ring. Experiments with rotation were conducted using a Motomatic motor generator. All solutions were deaerated by purging with argon for 10 min. All electrochemical experiments were performed at room temperature (21 ± 2 °C).

Immobilization of Hemin. A 0.5 mM hemin solution was prepared by dissolving 2.3 mg of hemin in 5 mL of a 0.01 M pH 10 buffer solution since hemin only dissolves in basic solution. Prior to use, the PG electrodes were abraded using 40 μm Al₂O₃ sandpaper and

- (16) Einsle, O.; Messerschmidt, A.; Huber, R.; Kroneck, P. M. H.; Neese, F. *J. Am. Chem. Soc.* **2002**, *124*, 11737–11745.
- (17) Armstrong, F. A. *J. Chem. Soc., Dalton Trans.* **2002**, 661–671.
- (18) Leger, C.; Elliott, S. J.; Hoke, K. R.; Jeuken, L. J. C.; Jones, A. K.; Armstrong, F. A. *Biochemistry* **2003**, *42*, 8653–8662.
- (19) Rusling, J. F.; Nassar, A. E. F. *J. Am. Chem. Soc.* **1993**, *115*, 11891–11897.
- (20) Nassar, A.-E. F.; Willis, W. S.; Rusling, J. F. *Anal. Chem.* **1995**, *67*, 2386–2392.
- (21) Nassar, A.-E. F.; Bobbitt, J. M.; Stuart, J. D.; Rusling, J. F. *J. Am. Chem. Soc.* **1995**, *117*, 10986–10993.
- (22) Lu, Z.; Huang, Q.; Rusling, J. F. *J. Electroanal. Chem.* **1997**, *423*, 59–66.
- (23) Bayachou, M.; Lin, R.; Cho, W.; Farmer, P. J. *J. Am. Chem. Soc.* **1998**, *120*, 9888–9893.
- (24) Mimica, D.; Zagal, J. H.; Bedioui, F. *Electrochem. Commun.* **2001**, *3*, 435–438.
- (25) Immoos, C. E.; Chou, J.; Bayachou, M.; Blair, E.; Greaves, J.; Farmer, P. J. *J. Am. Chem. Soc.* **2004**, *126*, 4934–4942.
- (26) Tao, N. J.; Cardenas, G.; Cunha, F.; Shi, Z. *Langmuir* **1995**, *11*, 4445–4448.
- (27) Sagara, T.; Fukuda, M.; Nakashima, N. *J. Phys. Chem. B.* **1998**, *102*, 521–527.
- (28) Arifuku, F.; Mori, K.; Muratani, T.; Kurihara, H. *Bull. Chem. Soc. Jpn.* **1992**, *65*, 1491–1495.
- (29) Shigehara, K.; Anson, F. C. *J. Phys. Chem.* **1982**, *86*, 2776–2783.
- (30) Jiang, R.; Dong, S. *Electrochim. Acta* **1990**, *35*, 1227–1232.
- (31) Nakashima, N.; Tokunaga, T.; Owaki, H.; Murakami, H.; Sagara, T. *Colloids Surf. A.* **2000**, *169*, 163–170.
- (32) Younathan, J. N.; Wood, K. S.; Meyer, T. J. *Inorg. Chem.* **1992**, *31*, 3280–3285.
- (33) Bedioui, F.; Trevin, S.; Albin, V.; Gomez Villegas, M. G.; Devynck, J. *Anal. Chim. Acta* **1997**, *341*, 177–185.
- (34) Lei, J.; Ju, H.; Ikeda, O. *Electrochim. Acta* **2004**, *49*, 2453–2460.
- (35) Hayon, J.; Ozer, D.; Rishpon, J.; Bettelheim, A. *J. Chem. Soc., Chem. Commun.* **1994**, 619–620.

- (36) Bedioui, F.; Bouchier, Y.; Sorel, C.; Devynck, J.; Coche-Guerrente, L.; Deronzier, A.; Moutet, J. C. *Electrochim. Acta* **1993**, *38*, 2485–2491.
- (37) Willsau, J.; Heitbaum, J. *J. Electroanal. Chem.* **1985**, *194*, 27–35.
- (38) Van der Plas, J. F.; Barendrecht, E. *Rec. Trav. Chim. Pays Bas* **1977**, *96*, 133–136.
- (39) Van den Brink, F.; Visscher, W.; Barendrecht, E. *J. Electroanal. Chem.* **1983**, *157*, 283–304.
- (40) Dean, J. A., Ed. *Lange's Handbook of Chemistry*, 14th ed.; McGraw-Hill: London, 1992; p 5.6.

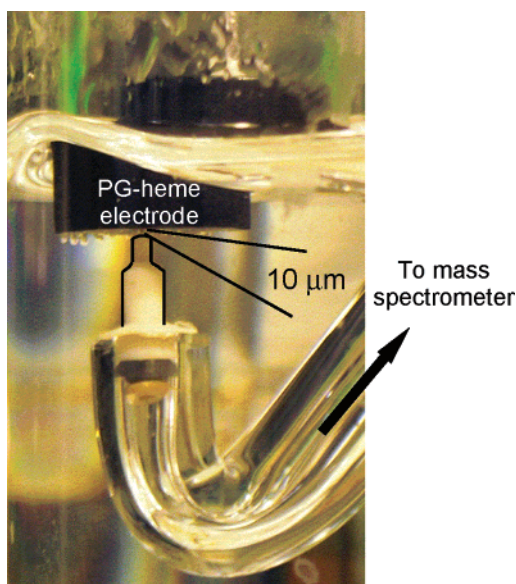


Figure 1. Photograph of OLEMS setup: a porous Teflon tip is in close contact ($d \sim 10 \mu\text{m}$) to the PG-heme electrode.

ultrasonicated in Millipore MilliQ water for 5 min. The electrode was dried in a N_2 stream for 10 s. The electrode was immersed in the hemin solution for 10 min to saturate the surface with hemin,^{41,42} after which the electrode was rinsed with water.

Rotating Ring Disk Electrode (RRDE) Experiments. Rotating ring disk electrodes were constructed as described previously^{38,39} and have a collection efficiency of 0.27 ± 0.03 . Prior to the measurements, the Pt ring was abraded together with the PG disk on $40 \mu\text{m}$ Al_2O_3 sandpaper and was also immersed in the 0.5 mM hemin solution. Subsequently, the Pt ring was cleaned by electropolishing: alternately a potential in the hydrogen evolution region (-0.8 V vs SCE) and a potential in the oxygen evolution region (1.5 V vs SCE) was applied for 5 s, which was repeated 25 times.

On-Line Electrochemical Mass Spectrometry (OLEMS). OLEMS measurements were performed on a Balzers Prisma QMS 200 mass spectrometer. The connection between the mass spectrometer and the cell was established through a steel capillary connected to a glass tube onto which a porous Teflon tip was attached. This tip was placed at approximately $10 \mu\text{m}$ from the PG-heme electrode surface as shown by the photograph in Figure 1. Details of the setup will be published elsewhere.⁴³ The electrode could not be rotated; hence, NO was continuously bubbled through solution to enhance NO mass transfer. Baseline values measured in a solution without NO were subtracted in NO reduction experiments.

Results

Prior to studying electrochemical NO reduction, we investigated the electrochemical properties of adsorbed heme groups on pyrolytic graphite. Figure 2a shows a voltammogram of a freshly prepared PG-heme electrode. The observed redox couple corresponds to the $\text{Fe}^{\text{III}}/\text{Fe}^{\text{II}}$ couple of the adsorbed heme groups. The redox couple has a midpoint potential $E_m = -0.42 \text{ V}$ versus SCE, which is the same as values of E_m previously reported for heme adsorbed on gold⁴⁴ and highly ordered pyrolytic

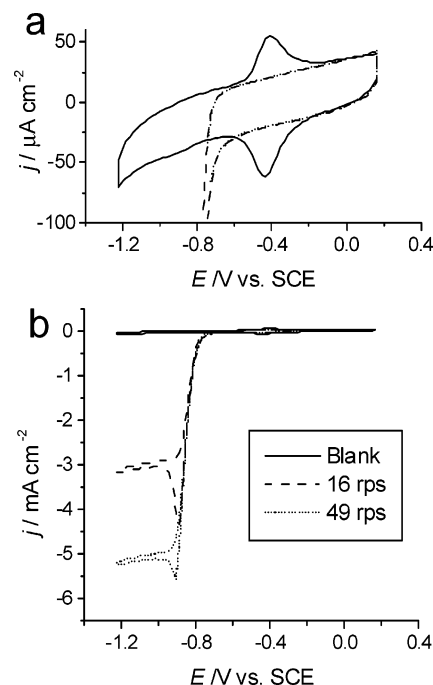


Figure 2. Cyclic voltammograms of a hemin-modified PG electrode in an NO free (—) and in a saturated NO solution at 16 rps (---) and 49 rps (·····). Note that panels a and b have different current scales. Buffer: 0.5 M phosphate, pH 7; scan rate = 500 mV/s.

graphite (HOPG).²⁷ E_m is not dependent on the pH of the solution below pH 4 but shows a dependence of -59 mV/pH above pH 5 (Supporting Information S1). This dependence can be ascribed to a proton transfer accompanying the electron transfer of the $\text{Fe}^{\text{III}}/\text{Fe}^{\text{II}}$ couple, possibly due to a ligand change from H_2O to OH^- upon oxidation of the iron center.^{29,44} A linear relation between the current density J_p and the scan rate ν was observed (Supporting Information S2), which indicates that the voltammetric response is due to a surface-confined species. Electron transfer between the graphite and the adsorbed heme groups is fast since the cathodic and anodic peak potentials do not depend on the scan rate ν for scan rates up to 10 V/s. As can be calculated from Laviron's theory,⁴⁵ this is in line with the previously obtained electron-transfer rate of $4.9 \times 10^3 \text{ s}^{-1}$.^{27,46} The amount of adsorbed hemin that can be calculated from the anodic peak charge is $1.5 \times 10^{-10} \text{ mol cm}^{-2}$. This is higher than for hemin adsorbed on HOPG (7.7×10^{-11}),^{27,46} which can be explained by the roughness of the pyrolytic graphite used.

Upon saturation of the solution with NO, a new reduction wave is observed starting at potentials around -0.75 V versus SCE (Figure 2b), which can be assigned to NO reduction by the adsorbed heme groups. Below -0.9 V versus SCE, the reaction rate of this reaction is limited by NO mass transfer, as can be deduced from the fact that the observed current is strongly dependent on the rotation rate of the electrode. It is important to note that the observed reduction waves are not influenced by nitrite, which is often observed in concentrated NO solutions. PG-heme electrodes are only able to reduce nitrite at low pH^{32,33} and are unable to do so at pH 7 (Supporting Information S3). Another effect of the saturation of the solution with NO is the disappearance of the $\text{Fe}^{\text{III}}/\text{Fe}^{\text{II}}$ couple from

(41) Brown, A. P.; Koval, C.; Anson, F. C. *J. Electroanal. Chem.* **1976**, *72*, 379–387.

(42) Duong, B.; Arechabaleta, R.; Tao, N. J. *J. Electroanal. Chem.* **1998**, *447*, 63–69.

(43) Wonders, A. H.; Housmans, T. H. M.; Rosca, V.; Koper, M. T. M. Submitted for publication.

(44) Pilloud, D. L.; Chen, X.; Dutton, P. L.; Moser, C. C. *J. Phys. Chem. B* **2000**, *104*, 2868–2877.

(45) Laviron, E. *J. Electroanal. Chem.* **1979**, *101*, 19–28.

(46) Feng, Z. Q.; Sagara, T.; Niki, K. *Anal. Chem.* **1995**, *67*, 3564–3570.

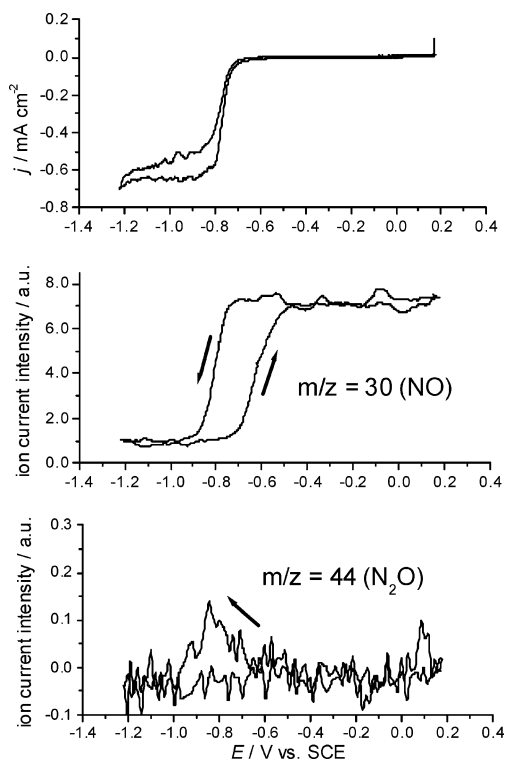


Figure 3. OLEMS measurements of adsorbed hemin in saturated NO solution. Top: cyclic voltammogram of adsorbed hemin. Middle: ion current intensity for $m/z = 30$ (NO) measured in the mass spectrometer as a function of potential. Bottom: ion current intensity for $m/z = 44$ (N_2O) measured in the mass spectrometer as a function of potential. Measurements were done in 0.5 M phosphate, pH 7.0 under continuous NO bubbling through the solution using a scan rate = 10 mV/s.

voltammetry (Figure 2a). This can be explained by NO binding to the heme group, which affects the reduction potentials of the $\text{Fe}^{\text{III}}/\text{Fe}^{\text{II}}$ couple. Both the Fe^{III} and the Fe^{II} state of the heme can bind NO.^{47,48}

The selectivity of the electrochemical NO reduction, which is the main focus of this study, cannot be directly derived from a voltammogram such as Figure 2. Therefore, voltammetry was combined with the OLEMS and RRDE techniques that can determine selectivity in situ. The OLEMS results are displayed in Figure 3, which shows the voltammetric response as well as the ion current intensities for $m/z = 30$ (NO) and $m/z = 44$ (N_2O) for electrochemical NO reduction. The observed voltammetric response is similar to NO reduction in other voltammetric experiments (Figure 2), even though the electrode could not be rotated. As soon as NO reduction occurred (around -0.8 V), a sharp decrease in the ion current intensity for $m/z = 30$ was observed, indicating that NO was consumed. A small increase in the ion current intensity for $m/z = 44$ was also observed, indicating the formation of a small amount of N_2O . However, contrary to the consumption of NO, the formation of N_2O was only observed at the start of the NO reduction and was not observed during continuous NO reduction at lower potentials. As was shown previously, the OLEMS setup is able to detect the formation of very small amounts of N_2O , and since the cell is purged with argon, CO_2 from air does not interfere with N_2O detection.⁴³ This is also evidenced by the small

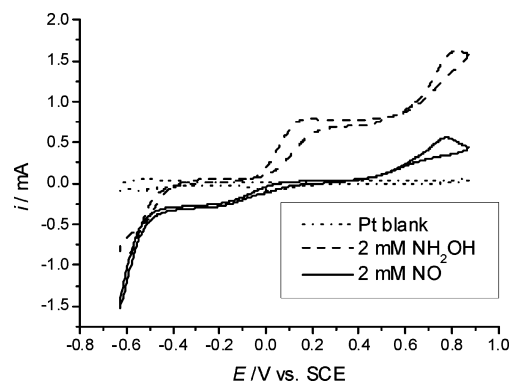


Figure 4. Cyclic voltammograms of a Pt-ring in the absence (.....) and in the presence of 2 mM NO (—) or 1 mM $(\text{NH}_3\text{OH})_2\text{SO}_4$ (---). Buffer: 0.5 M phosphate, pH 7.0; scan rate = 50 mV/s; 16 rps.

amount of CO_2 that can be detected during methanol oxidation on a platinum single-crystal electrode⁴³ and by the very small amounts of N_2O measured during hydroxylamine oxidation on a polycrystalline platinum electrode utilizing a similar DEMS setup, in complete accordance with results from independent FTIR measurements.⁴⁹ As the sensitivities for NO and N_2O are similar in the mass spectrometer, the relatively small N_2O signal that is observed implies that N_2O is only a minor byproduct at the start of the NO reduction. N_2 ($m/z = 28$), another possible product of NO reduction by PG-heme, was never observed in our OLEMS experiments, indicating that the main reaction product of the NO reduction is either NH_2OH or NH_3 . These products are difficult to observe with OLEMS because they are not gaseous and their fragmentation products have ion current intensities close to those of water.

RRDE⁵⁰ was employed to detect the possible formation of NH_2OH and NH_3 . For the ring to be used for selectivity measurements, the voltammetric responses of the possible products (NH_2OH and NH_3) and of the reactant (NO) on Pt have to be known. Therefore, cyclic voltammetry was performed with NO, NH_2OH , and NH_3 in solution (Figure 4). NH_3 could not be oxidized within our potential window, which agrees with previous observations that ammonia oxidation on Pt only occurs in alkaline solution.⁵¹ NH_2OH exhibits an oxidation wave starting at 0 V versus SCE, and NO exhibits a reduction wave starting at 0 V versus SCE. The fact that reduction of NH_2OH occurs at much lower potentials and that oxidation of NO occurs at much higher potentials allows for a straightforward distinction between NO and NH_2OH on the Pt ring.

Figure 5 shows the voltammetric response of the Pt ring during NO reduction on the PG-heme disk as compared to the voltammetric response of the Pt ring in saturated NO solution without NO reduction on the disk. When NO is reduced on the disk (at $E_{\text{disk}} = -0.9$ V, $i_{\text{disc}} = -1.5$ mA), a decrease of approximately 0.14 mA was observed in the NO reduction wave on the ring. On the Pt ring, NO is reduced via a one-electron process to N_2O^3 at potentials between -0.2 and -0.4 V versus SCE. Assuming that NO is reduced to NH_2OH on the disk, the observed decrease in current of 0.14 mA corresponds to a collection efficiency of 0.28, which is in agreement with the

(47) Hoshino, M.; Ozawa, K.; Seki, H.; Ford, P. C. *J. Am. Chem. Soc.* **1993**, *115*, 9568–9575.

(48) Hoshino, M.; Maeda, M.; Konishi, R.; Seki, H.; Ford, P. C. *J. Am. Chem. Soc.* **1996**, *118*, 5702–5707.

(49) Rosca, V.; Beltramo, G. L.; Koper, M. T. M. *J. Electroanal. Chem.* **2004**, *566*, 53–62.

(50) Bard, A. J.; Faulkner, L. R. *Electrochemical Methods: Fundamentals and Applications*; 2nd ed.; John Wiley & Sons: New York, 1980; pp 311–367.

(51) Gerischer, H.; Mauerer, A. *J. Electroanal. Chem.* **1970**, *25*, 421–433.

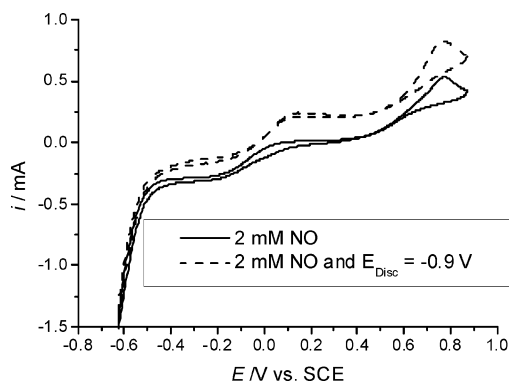


Figure 5. Cyclic voltammograms of Pt-ring in saturated NO (2 mM) solution (—) and in saturated NO solution with a potential of -0.9 V (---) applied to the PG-heme disk. Buffer: 0.5 M phosphate, pH 7.0; scan rate = 50 mV/s; 16 rps. The recorded current on the disk was -1.5 mA.

collection efficiency of 0.27 ± 0.03 previously reported for this electrode.^{38,39} This also confirms that N_2O is not the main product of NO reduction on the disk since this would imply an unrealistically low collection efficiency of only 0.09. The decrease in the NO reduction wave is accompanied by an increase of ca. 0.21 mA at potentials above 0 V. Comparison of Figures 4 and 5 suggests that this increase is due to the oxidation of NH_2OH , implying that NH_2OH is formed as a product on the PG-heme disk. It is difficult to determine quantitatively from these measurements whether NO reduction is 100% selective toward NH_2OH since for this we need to know the number of electrons transferred in NH_2OH oxidation on the Pt ring. However, the oxidation of NH_2OH on Pt in neutral media is known to result in the formation of more than one product (NO , N_2O , N_2)^{52–54}; therefore, this number can range between 1 and 3. In our case, assuming that NH_2OH is the only product of NO reduction on the disk, the increase in the current of 0.21 mA corresponds to a calculated number of electrons of approximately 1.5. This is plausible and suggests that NH_2OH on the ring is oxidized to a combination of N_2 and N_2O .

OLEMS and RRDE strongly suggest that NH_2OH is the main reaction product of NO reduction at a PG-heme electrode, and this can be confirmed by indirect but quantitative evidence from voltammetry. One such experiment is comparing NO reduction on a PG-heme electrode to NO reduction on a Pt electrode constructed in exactly the same way, such that both electrode geometries exhibit the same NO mass transfer behavior. It is known that NO reduction on Pt leads to N_2O as the only product at potentials between -0.2 and -0.4 V versus SCE³ and that the reaction rate is limited by NO mass transfer. On a PG-heme disk, NO mass transfer also limits the NO reduction at potentials below -0.9 V. Both mass transfer limited currents are compared in Figure 6. On the Pt disk, a current of 1.63 mA cm^{-2} was observed, whereas on the PG-heme disk, a current of 4.92 mA cm^{-2} was observed, which is almost exactly three times the mass transfer limited current observed on Pt. Since the reduction of NO to N_2O on Pt corresponds to a one-electron transfer, the reduction on the PG-heme disk must correspond to a three-electron transfer. This implies that NO is reduced to NH_2OH and that the selectivity is very close to 100%.

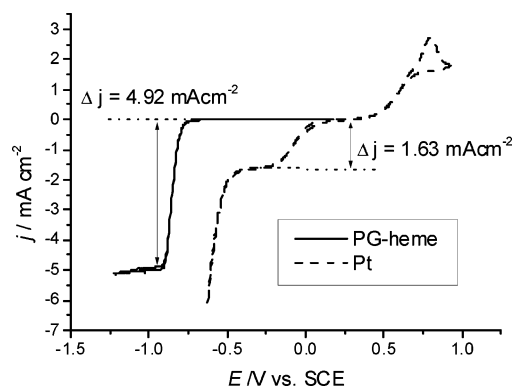


Figure 6. Cyclic voltammograms of adsorbed hemin on PG (—) and Pt (---) in saturated NO solution. Electrodes have the same geometry. Buffer: 0.5 M phosphate, pH 7.0; scan rate = 50 mV/s; 49 rps.

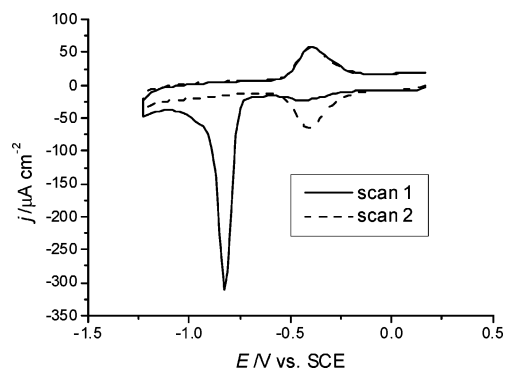


Figure 7. NO stripping voltammetry of adsorbed hemin. Scan 1 (—) and scan 2 (---). Buffer: 0.5 M phosphate buffer, pH 7.0; scan rate = 500 mV/s.

Calculation of the number of electrons transferred in a so-called NO stripping experiment also confirms the almost 100% selective formation of NH_2OH . Such an experiment is performed by reducing the Fe^{II} –NO adduct of the adsorbed heme groups without NO present in solution. The Fe^{II} –NO adduct was formed by performing continuous NO reduction on the PG-heme electrode for a short time (5 s) and transporting it to a buffer solution without NO. The Fe^{II} –NO adduct formed is stable in aerobic buffer solution for at least 10 min. The first two voltammetric scans recorded after transfer to the NO free buffer solution are shown in Figure 7. A reduction peak is observed in the first scan, which coincides with the reduction peak for continuous NO reduction (Figure 2). After this reduction peak, the Fe^{III}/Fe^{II} couple reappears, and in the second scan, no NO reduction peak is observed. The area under the reduction peak corresponds to a charge equivalent to 5.4×10^{-10} mol cm^{-2} . From the Fe^{III}/Fe^{II} couple, a heme coverage of 1.8×10^{-10} mol cm^{-2} can be calculated. The ratio of $\sim 3:1$ again indicates that three electrons are transferred per heme group, implying that NH_2OH is the main reaction product. The fact that the NO stripping peak coincides with the continuous NO reduction wave suggests similar mechanisms for continuous NO reduction and the NO stripping experiment.

The observation that the selectivity of NO reduction on PG-heme toward NH_2OH is very close to 100% suggests that the heme group is not able to break the N–O bond in NH_2OH . We investigated NH_2OH reduction by PG-heme, which showed that NH_2OH could be reduced by PG-heme (Supporting Information S3) but that the rate is much slower than NO reduction. This

(52) Karabinas, P.; Wolter, O.; Heitbaum, J. *Ber. Bunsen-Ges. Phys. Chem.* **1984**, *88*, 1191–1196.

(53) Moeller, D.; Heckner, K. H. *Z. Phys. Chem.* **1972**, *251*, 81–102.

(54) Davis, D. G. *Anal. Chem.* **1963**, *35*, 764–765.

indicates that breaking the N–O bond is indeed difficult although not impossible.

The fact that NH_2OH and not N_2O is the main product of the electrochemical NO reduction by PG-heme prompts a more detailed study of the reduction mechanism. To this end, we constructed Koutecky–Levich and Tafel plots⁵⁰ from the voltammetric RDE experiments to provide information about the rate-determining step in the mechanism and the possible involvement of reaction equilibria (Figures 8 and 9). We also investigated pH dependence. Data for the Koutecky–Levich plots can be obtained by performing chronoamperometric measurements at different rotation rates at potentials between -0.7 and -0.9 V. At these potentials, the reaction rate is determined by both reaction kinetics and NO mass transfer. A Tafel plot was constructed from the kinetically limiting currents at different potentials, which were determined by extrapolating the Koutecky–Levich plots to infinite rotation rate (i.e., $\omega^{-1/2} \rightarrow 0$). Kinetically limiting currents could only be determined for potentials of -0.81 V and higher since accurate determination at more negative potentials is hampered by nonlinear Koutecky–Levich plots, which are probably related to saturation of the heme groups by NO. At full saturation, the current will not increase with higher rotation rate ($\omega^{-1/2} \rightarrow 0$). The rotation rate at which the nonlinearity sets in depends on the applied potential since reduction of the heme–NO adduct becomes faster with decreasing potential. At high potentials (greater than -0.8 V), the heme group is almost saturated for all rotation rates, which makes it relatively straightforward to extrapolate the kinetically limiting current. At lower potentials, nonlinear Koutecky–Levich plots are observed, indicating that the heme groups become saturated with increasing rotation rate.

The slope determined from the Tafel plot (Figure 9) is 62 mV/dec, which can be interpreted in terms of a mechanism in which an electrochemical equilibrium is followed by a chemical rate-determining step (EC-mechanism).⁵⁵ The slope of the Tafel plot does not depend on the pH of the solution, indicating that the rate-determining step does not change with pH. Since the kinetically limiting current is directly related to the turnover number (number of reacted molecules per reactive center per second), the exponential relation between the kinetically limiting current and the potential in the Tafel plot implies that the turnover number depends exponentially on potential.

The pH dependence of the NO reduction was determined by plotting the potential at which a steady-state current of 0.6 mA cm^{-2} was measured versus the pH of the solution (Figure 10). This value of 0.6 mA cm^{-2} was chosen as it is relatively small as compared to the current observed when the reaction is completely limited by NO mass transfer (3 mA cm^{-2}) so that the influence of different diffusion parameters in the different buffer solutions was avoided. In contrast to the Tafel slope, the NO reduction rate is pH dependent, indicating that proton transfer plays an important role in the rate-determining step of the reaction. Surprisingly, however, the observed slope of -42 mV/pH significantly differs from the value of -59 mV/pH that is expected for one proton transfer per electron transfer.

Discussion

Electrochemical NO reduction by PG-heme results in the formation of NH_2OH as the main product. This can be concluded

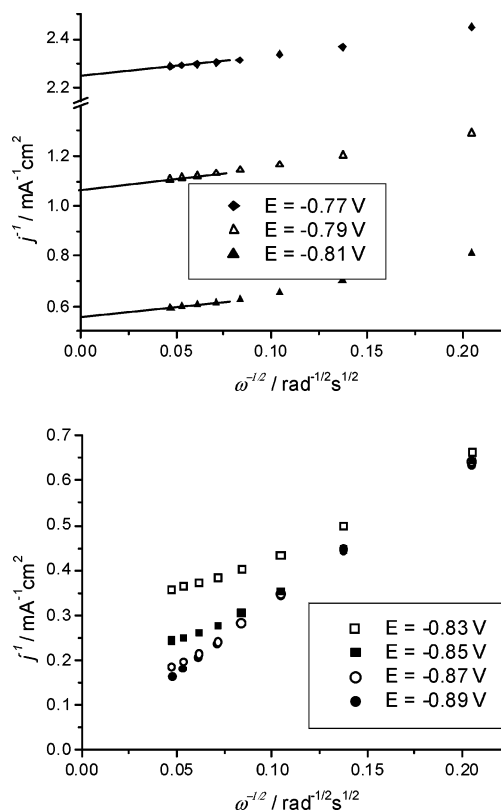


Figure 8. Koutecky–Levich plots of adsorbed hemin in saturated NO solution at $E = -0.77$ V (\blacklozenge), $E = -0.79$ V (\triangle), $E = -0.81$ V (\blacktriangle), $E = -0.83$ V (\square), $E = -0.85$ V (\blacksquare), $E = -0.87$ V (\circ), and $E = -0.89$ V (\bullet). Buffer: 0.5 M phosphate buffer, pH 7.0. Kinetically limiting currents were determined by drawing a line through the four points with the highest rotation rates and extrapolating to the j^{-1} -axis as indicated in the figure.

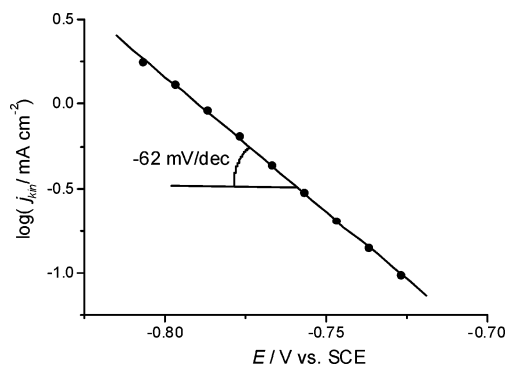


Figure 9. Tafel plot of adsorbed hemin in saturated NO solution. Buffer: 0.5 M phosphate, pH 7.0.

from (i) the OLEMS measurements that did not show the formation of significant amounts of N_2O and N_2 , (ii) the RRDE experiments that showed the oxidation of NH_2OH on the Pt ring, (iii) the comparison to NO reduction on Pt that showed that three electrons are consumed in the NO reduction on the PG-heme electrode, and (iv) the stripping experiments that also showed that three electrons are involved in the reduction of heme-bonded NO.

N_2O was observed as a minor product in the OLEMS experiment. This suggests that there are two competing pathways for NO reduction, one leading to the formation of NH_2OH and one leading to the formation of N_2O . The mechanism by which N_2O is formed is probably similar to the mechanism previously reported for NO reduction by immobilized myoglobin and

(55) Vetter, K. J. *Elektrochemische Kinetik*; Springer-Verlag: Berlin, 1961; pp 302–357.

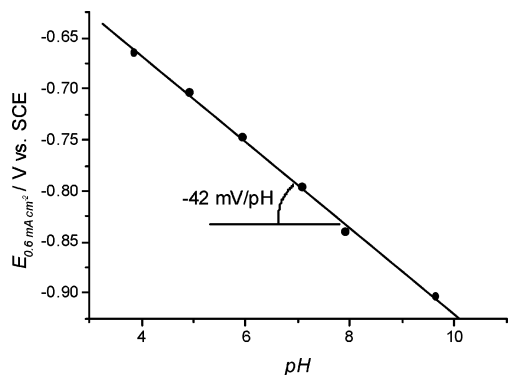
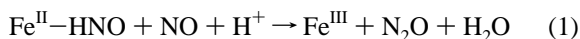
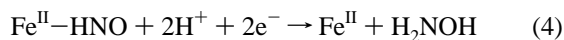
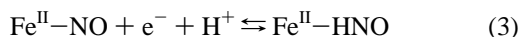


Figure 10. Potential at which a steady-state current of 0.6 mA cm^{-2} is measured as a function of pH in saturated NO solution. Buffer: 0.5 M acetate, phosphate, or borate; 16 rps.

hemoglobin: it proceeds via an $\text{Fe}^{\text{II}}\text{-HNO}$ adduct, which has been observed for myoglobin in solution,^{12,56,57} and subsequently reacts with NO to form N_2O (eq 1).



The main reaction pathway in our system, however, leads to the formation of NH_2OH and hence occurs via another mechanism. The Tafel slope of 62 mV/dec and the pH dependence of -42 mV/pH suggest an EC mechanism (i.e., an electrochemical equilibrium followed by a chemical step) combined with proton transfer. On the basis of this information, we postulate a mechanism for the NH_2OH formation (eqs 2–4). The first two steps are identical to the mechanism in which N_2O is formed and also result in the formation of an $\text{Fe}^{\text{II}}\text{-HNO}$ intermediate. Subsequently, the $\text{Fe}^{\text{II}}\text{-HNO}$ adducts react further to NH_2OH (eq 4). Note that eq 4 is an overall reaction—in the EC mechanism, the rate-determining step is chemical and should not involve electron transfer. It would be premature to speculate on the nature of the chemical step and how the involvement of proton transfer could lead to the unusual pH dependence.



This mechanism suggests that the $\text{Fe}^{\text{II}}\text{-HNO}$ adduct is the branching point between the pathway leading to N_2O and the pathway leading to NH_2OH . This raises the question as to why our system favors the pathway to NH_2OH and why other systems such as NO reduction by cytochrome P450nor favor the pathway to N_2O . This question is difficult to answer since most likely there are a number of factors that can influence the preference for one or the other pathway. These probably include the residues surrounding the heme group, the mode of electron transfer to the heme group, the way in which a second NO molecule can bind to the active site, and the pH of the solution.

A comparison to enzymatic NO reduction shows that the way in which the electrons are provided to the catalytic center of

the enzyme can have a profound influence on selectivity. The reason that NO reduction catalyzed by cytochrome P450nor leads to N_2O and not NH_2OH may be tentatively related to the fact that the electron donor NADH can only provide two electrons. The transfer of more electrons from a second NADH is unlikely since only one NADH can bind close to the heme.⁵⁸ This implies that NH_2OH formation is impeded due to lack of electrons; therefore, $\text{Fe}^{\text{II}}\text{-HNO}$ can only react to N_2O . Interestingly, the nitrite reduction by cytochrome *c'* nitrite reductase also proceeds via an $\text{Fe}^{\text{II}}\text{-HNO}$ intermediate, which reacts via NH_2OH to NH_3 ,¹⁶ showing that reduction of the $\text{Fe}^{\text{II}}\text{-HNO}$ adduct to NH_2OH by an enzyme is possible. Cytochrome *c'* nitrite reductase has five heme groups that can provide more electrons, and further reduction of the $\text{Fe}^{\text{II}}\text{-HNO}$ adduct is therefore not impeded by a limited availability of electrons. However, sufficient availability of electrons does not necessarily imply that NH_2OH is the reaction product. NO reduction by immobilized heme proteins results in the formation of N_2O , even though further reduction of the $\text{Fe}^{\text{II}}\text{-HNO}$ adduct should be possible in these systems since the electrode can provide an unlimited number of electrons. In contrast to NO reduction by adsorbed heme groups, the pathway to N_2O is apparently favored over the pathway to NH_2OH . This implies that the specific surroundings of the heme group also have a profound influence on selectivity.

Another important observation from this study is that NH_3 was not observed as a product in NO reduction by PG-heme. Our experiments show that electrocatalytic reduction of NH_2OH is possible, but it is much slower than NO reduction, which suggests that NO bond breaking by adsorbed heme groups is very sluggish. This is in contrast to transition metals such as $\text{Pt}^{3,4}$ and Pd^5 on which NO reduction has been shown to result in the formation of N_2O , N_2 , NH_2OH , and NH_3 depending on both the kind of metal used and the potential applied. Significantly, NO adsorbed on Pt without NO in solution can only be reduced to NH_3 and not to N_2O and NH_2OH .⁵⁹ Interestingly, NH_2OH was also observed as the main product in electrocatalytic reduction of NO by adsorbed iron-phthalocyanine,⁶ which suggests that adsorbed iron complexes are poor catalysts for reducing NO to NH_3 . An explanation could be that N–O bonds can only be broken at significant rates when at least two adjacent adsorption sites are available. This is supported by the fact that NH_3 formation on most metals is only possible if the adsorbed NO has space to tilt to a bridging configuration (as illustrated in Figure 11).⁶⁰ Since a heme group has only one iron center, such a bridging confirmation cannot be achieved; therefore, N–O bond breaking is very sluggish.

The selectivity of NO reduction by adsorbed heme confirms that this is an intermediate system between NO reduction on bare metal electrodes and enzymes, whether immobilized on electrodes or not. Figure 11 gives a schematic representation in which NO reduction by enzymes, adsorbed heme complexes, and metal electrodes are compared.

Conclusion

We have shown that adsorbed heme groups reduce NO to NH_2OH with a selectivity of almost 100%. A small amount of

(56) Sulc, F.; Fleischer, E.; Farmer, P. J.; Ma, D.; La Mar, G. N. *J. Biol. Inorg. Chem.* **2003**, *8*, 348–352.

(57) Sulc, F.; Immoos, C. E.; Pervitsky, D.; Farmer, P. J. *J. Am. Chem. Soc.* **2004**, *126*, 1096–1101.

(58) Park, S.-Y.; Shimizu, H.; Adachi, S.-I.; Nakagawa, A.; Tanaka, I.; Nakahara, K.; Shoun, H.; Obayashi, E.; Nakamura, H.; Iizuka, T.; Shiro, Y. *Nat. Struct. Biol.* **1997**, *4*, 827–832.

(59) Beltramo, G. L.; Koper, M. T. M. *Langmuir* **2003**, *19*, 8907–8915.

(60) Brown, W. A.; King, D. A. *J. Phys. Chem. B* **2000**, *104*, 2578–2595.

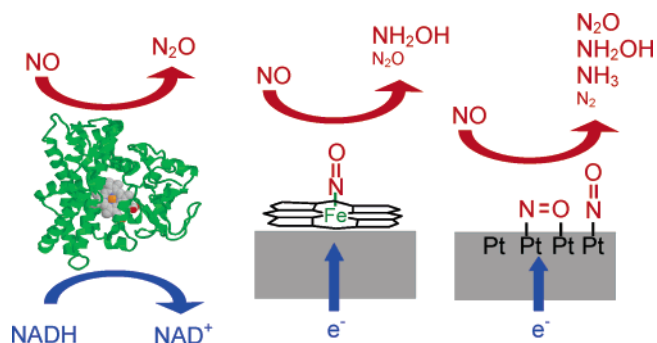


Figure 11. Schematic overview of the selectivity of NO reduction by P450nor, adsorbed heme, and metal surfaces.

N_2O was also observed at high potentials, indicating that there is competition between an NO reduction pathway to NH_2OH and a pathway to N_2O . However, the pathway to NH_2OH is

clearly favored at low potentials. Adsorbed heme provides an interesting new system for mechanistic study of NO reduction that can help in obtaining a better understanding of the factors that govern selectivity in both biological NO reduction and inorganic NO reduction.

Acknowledgment. This work was supported by the National Research School Combination Catalysis (NRSC-C).

Supporting Information Available: Plots of the midpoint potentials of adsorbed hemin as a function of pH, the peak currents of adsorbed hemin as a function of scan rate, and cyclic voltammograms of adsorbed hemin in the presence of hydroxylamine and nitrite. This information is available free of charge via the Internet at <http://pubs.acs.org>.

JA051151A